

TUNABLE X-RAY SOURCE BASED ON MOSAIC CRYSTALS USING FOR MEDICINE APPLICATIONS

D.A. BAKLANOV, R.A. SHATOKHIN, I.E. VNUKOV*, YU.V. ZHANDARMOV

Belgorod State University, 14 Studencheskaya str., 308007 Belgorod, Russia

**E-mail: vnukov@bsu.edu.ru*

N.I. MASLOV, A.A. MAZILOV

National Science Center "Kharkov Institute of Physics and Technology",

61108 Kharkov, Ukraine

The prospect of creation of the X-ray source with tunable wavelength on the base of a middle energy accelerator and mosaic crystals are analyzed. It is proved, that due to the contribution of diffracted bremsstrahlung, the mosaic crystals provide the essentially greater yield of hard radiation ($\omega \geq 20$ keV), than perfect crystals. It is shown, that using a traditional scheme with one crystal for X-ray generation isn't acceptable for medicine applications. Double-crystal scheme is offered and analyzed, in which one crystal is located on the electrons beam, and another is used for monochromatization and parallel moving of the X-ray beam. It provides suppression of background bremsstrahlung, and there is no need to move the object when change the photons energy.

Keywords: X- and gamma-ray sources, mirrors, gratings, and detectors

1. Introduction

Parametric X-ray (PXR) production by high-energy charged particles penetrating through a crystal has been extensively studied in the past two decades (see, e.g.,^{1,2} and references therein). The interest to this radiation is caused by the search for new high-intensity, tunable X-ray sources, capable to offer an alternative to storage rings. Advantages of PXR over other sources, based on the use of radiation of fast particles in substance, is the opportunity to vary the energy of photons by the change of orientation of a crystal or a position of the radiated object and smaller dose loadings on PXR is let out at the big angles to the direction of an electron beam.

To a first approximation PXR can be viewed as the coherent dipole emission of proper electromagnetic field of a particle on the electron shells of

periodically arranged atoms of a crystal.^{3,4} It is supposed that the most perspective is the use of this type of radiation in medical purposes, where small sources of hard quasimonochromatic X-ray ($\omega \geq 20$ keV, $\Delta\omega/\omega \leq 5\%$)⁵ are demanded for the transmission radiography and K-edge angiography^{6, 8}

Measuring of the PXR characteristics, performed for almost all conventional crystals with perfect structure: diamond, silicon, germanium, tungsten, quartz, lithium fluoride (see^{1,2} and references therein) showed that the radiation yield weakly depends on the crystal and is not enough for the practical realization of the source, based on this mechanism of radiation. The ways of increase of radiation yield, offered recently (see^{7,9,10} and references therein) also hasn't found practical application. The use of X-ray mirrors as a targets⁹ and multi-layer crystal targets⁷ demands the electron energy $E_e \geq 500$ MeV that is comparable with the storage rings and economically is not profitable. Multiple passes of electrons through the X-ray mirror or thin crystalline target in the cyclic accelerator¹⁰ is accompanied by enlarging the angle of multiple scattering and loosing of the particles on the walls of the accelerating chamber. The radiation yield registered during such measurements, is compared with that is obtained with the usual thickness of targets in the PXR experiments (~ 1 mm).

In works^{11,12} it is noted that the use of mosaic crystals permits to increase the radiation yield due to the contribution of diffracted photons of the bremsstrahlung (DB). In quoted works the DB contribution to the yield of the registered radiation in some times exceeded the PXR contribution and was well described by the theory of X-ray diffraction in mosaic crystals¹³. Accordance of the results of the measuring for the mosaic crystals of pyrolytic graphite¹¹ and diamond¹² with the calculation allows to compare perfect and mosaic crystals from the point of view of their use for generation of hard X-ray emission and appreciate possible advantages and disadvantages.

2. General expressions

As it is shown in the range of the experimental works (see e.g.¹⁴ and references therein) kinematic PXR theory describes the measuring results for the energies of electrons from some MeV to GeV with the fault not worse than 10-15%, that is why to count the PXR yield the formula of spectral and angular distribution, obtained by the kinematical approach in the work¹⁵ is used:

$$\frac{d^2 N}{dZ d\Omega} = \frac{\sum_{\nu} \alpha \omega^3 |\chi_{\vec{g}}|^2}{2\pi \epsilon_0^{3/2} \beta (1 - \sqrt{\epsilon_0} \vec{\beta} \vec{n})} \left[\frac{(\omega \vec{\beta} - \vec{g}) \vec{e}_{\vec{k}\nu}}{(\vec{k}_{\perp} + \vec{g}_{\perp})^2 + \frac{\omega^2}{\beta^2} \{\gamma^{-2} + \beta^2 (1 - \epsilon_0)\}} \right]^2 \quad (1)$$

The system of units used is $\hbar = m_e = c = 1$. Here $\epsilon_0 = 1 - \omega_p^2/\omega^2$, where ω_p - plasma frequency of medium, $\vec{\beta} = \beta \vec{n}_0$ - vector of electron speed, \vec{n}_0 , \vec{n} - unit vectors in the line of the flying electron and radiated photon (with energy ω and momentum \vec{k}), \vec{g} - vector of reciprocal lattice, $\vec{e}_{\vec{k}\nu}$ polarized vectors, $\vec{e}_{\vec{k}1} = \frac{[\vec{n}, \vec{n}_0]}{|\vec{n}, \vec{n}_0|}$, $\vec{e}_{\vec{k}2} = [\vec{e}_{\vec{k}1}, \vec{n}]$, \perp index, indicated the projections of vectors on the plane, square with no. The other notation is conventional. The term $|\chi_{\vec{g}}|^2$ denotes the following value:

$$|\chi_{\vec{g}}|^2 = |S(\vec{g})|^2 \exp(-2W) \left[-\frac{\omega_p^2 f(\vec{g})}{\omega^2 z} \right]^2 \quad (2)$$

Here $|S(\vec{g})|^2$ is the structure factor, $\exp(-2W)$ is the Debye - Waller factor, $f(\vec{g})$ is the Fourier component of the spatial distribution of electrons in a crystal atom ($f(0) = Z$, where Z is the number of electrons in an atom), calculated according to the results¹⁶.

The dependence of PXR spectral and angular distribution on the angle between the direction of electron movement and the crystal plane is considered in accordance with the method, proposed in the work¹⁷. The divergence of the electron beam inside the crystal and absorption of the PXR photons were calculated by the method, described in.^{11,22} The crystal mosaicity was taken into account by the calculation of the spectrum for different mosaic blocks, taking into account their distribution in the target.

The main advantage of mosaic crystals is the additional contribution to the registered spectrum of diffracted real photons. For the electrons of medium energy ($E_e \leq 100$ MeV) the main photon source is the bremsstrahlung (BS). For the relativistic electron and soft photons ($\omega \ll E_e$) the spectral and angular distribution of BS intensity produced per unit of path length in an amorphous substance can be represented in the form¹⁸:

$$\frac{d^2 I}{d\omega d\Omega} = \frac{\gamma^2}{\pi L} \frac{1 + \gamma^4 \theta^4}{(1 + \gamma^2 \theta^2)^4} \quad (3)$$

where L is the radiation length, θ - angle of photon outlet.

In the analyzed case in the crystal the divergent photon beam with continuous spectrum occurs. To reflect a monodirect and monochromatic

photon beam from the element of mosaic crystal with volume ΔV can be noted¹³ as:

$$\int P(\theta) d\theta = Q\Delta V, \quad (4)$$

where $P(\theta)$ - reflecting power of the crystal element at the angle θ , which is proportionate to the distribution of mosaic blocks in the crystal¹⁹. $Q\Delta V$ - integral reflection from the element ΔV , where Q - the integrated reflectivity, depends on the crystal parameters and the radiant energy in the following way:

$$Q = \left(\frac{e^2}{mc^2} \right)^2 \frac{N^2 \lambda^3}{\sin(2\Theta)} |F_p| |F(\vec{g})|^2, \quad (5)$$

where N - atom concentration, $|F(\vec{g})|^2 = |S(\vec{g})|^2 \cdot |f(\vec{g})|^2 \cdot \exp(-2W)$, λ - wavelength, $|F_p|$ - polarization multiplier. If the polarization vector is perpendicular to the diffraction plane, $|F_p| = 1$; otherwise $|F_p| = \cos^2 2\Theta_B$. For an unpolarized photon beam $|F_p| = (1 + \cos^2 2\Theta_B)/2$. Here Θ_B is the angle between the crystallographic plane and the average direction of photon beam propagation.

Let the radiation with the spectral and angular intensity distribution $I(\omega, \vec{n})$ be incident on a mosaic crystal possessing the distribution of reciprocal lattice vectors $P(\vec{g})$ where ω and \vec{n} are the energy and the unit vector directed along the photon momentum vector, respectively. Here $\vec{g} = |\vec{g}|\vec{\alpha}$, where $\vec{\alpha}$ is the unit vector specifying the deflection of crystal micro blocks from the average direction $\vec{g}_0 = \langle \vec{g} \rangle$. The vector \vec{g}_0 is perpendicular to a crystal plane. It is rotated through the angle $(\pi/2 - \Theta_B)$ about the beam axis. The diffraction plane is determined by vectors \vec{n}_0 and \vec{g} .

Starting from Bragg's law for the photon with energy ω and direction \vec{n} we can formulate the requirement for the direction of vector \vec{g} of micro block, on which this photon can diffract.

$$\omega = \frac{\vec{g}\vec{n}}{\sqrt{\epsilon_0}(1 - \vec{n}'\vec{n})} = \frac{|\vec{g}|\sin\Theta}{\sqrt{\epsilon_0}(1 - \cos 2\Theta)}, \quad (6)$$

where \vec{n}' - vector, describing the direction of diffracted photon. Hence the angle between the directions of vectors \vec{n} and \vec{g} should meet the condition:

$$\sin\Theta = \frac{|\vec{g}|}{2\omega\sqrt{\epsilon_0}} \quad (7)$$

In the mosaic crystal this condition is met by the whole set of mosaic blocks which are suitable for the form:

$$\sin \Theta = \frac{(\vec{g}\vec{n})}{|\vec{g}|} = \frac{n_x g_x + n_y g_y + n_z g_z}{|\vec{g}|} \quad (8)$$

By this form we can define mosaic blocks, on which this photon can diffract and define the driving direction of the reflected photon \vec{n}' .

Then probability density of the reflection of photon with fixed ω and \vec{n} in the block of mosaic crystal with the thickness Δt along the photon driving direction can be written such:

$$f(\omega, \vec{n}) = q(\omega, \vec{n})Q(\omega)\Delta t, \quad (9)$$

where $q(\omega, \vec{n})$ - a factor of the crystal mosaicity:

$$q(\omega, \vec{n}) = \int P_m(\alpha_x(\omega, \vec{n}, \alpha_y), \alpha_y) d\alpha_y. \quad (10)$$

Here $P_m(\alpha_x, \alpha_y)$ - distribution of crystal mosaicism, expressed through $\omega, \vec{n}, \alpha_y$ in accordance with the forms ((5)-(7)).

To calculate the yield of the diffracted photons in the aperture of the collimator for each order of the reflection i , spectrum and angle distribution of the radiation intensity, taking into account multiple electron scattering in the target $\frac{d^2 I(\omega, \vec{n})_{BS}}{d\omega dt}$, was reduced with the probability density of the diffraction by all variables, including energy, angles of photon outlet θ_x and θ_y and crystal thickness:

$$Y_i = \int_{\Delta\omega_i} d\omega \int_T dt \iint_{\Delta\Omega} \frac{d^2 I(\omega, \vec{n})_{BS}}{d\omega dt} S(\omega, \vec{n}, \vec{n}', t) Q(\omega) q(\omega, \vec{n}) d\theta_x d\theta_y, \quad (11)$$

Here $S(\omega, \vec{n}, \vec{n}', t)$ - factor considering the radiation absorption in the target material and the experiment geometry, T - crystal thickness, $\Delta\Omega$ angle acceptance, and $\Delta\omega_i$ energetic capture of the detector for i reflection order, which depends on the collimation angle and radiation angular distribution.

According to the kinematic PXR theory for the definitely Bragg's direction the intensity of radiation is equal to zero.^{3,4,15} That is why in perfect crystals diffraction of PXR photons usually is not viewed. In the mosaic crystals for the photon, produced in one of the mosaic blocks, the diffraction conditions in other block can be fulfilled. To take into account this effect

for each PXR photon with the energy ω and momentum k from Bragg's law in accordance with (6)-(10) the blocks of mosaic, on which this photon can diffract, and the probability of reflection were defined. From here, taking into account the distribution of the mosaic blocks, PXR photon beam attenuation on its way from the birth point to the outlet out of crystal was defined. The second diffraction of the reflected photons of bremsstrahlung on the way from diffraction area to the outlet out of crystal was calculated similarly. More detailed the method of calculation of the PXR yield in the mosaic crystals was described in detail in.^{11,22}

3. Traditional scheme

The PXR yield linearly depends on the thickness of the crystal, that is why the natural way to increase the intensity is to enlarge the thickness of a target. On Figure 1 there is a calculated dependence of PXR yield for the reflection (220) and $\Theta_B = \Theta_D/2$ from the thickness of the silicon crystal. The calculation was conducted for the following conditions: the electron energy $E_e = 45$ MeV, electron beam divergence $\vartheta_e = 1.5$ mrad, the radiated object is at the angle $\Theta_D = 16.7^\circ$ ($\omega \sim 33$ keV). The round collimator with the diameter 5 mm is 3 meters far from the crystal ($\vartheta_{PXR} = 0.85$ mrad).

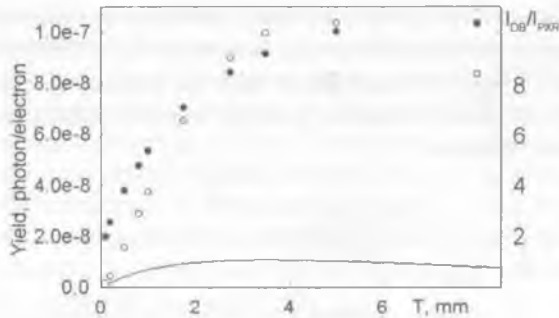


Fig. 1. The dependence of PXR and DB intensity on the silicon crystal thickness. Curve - PXR, \circ - DB, \bullet - Y_{DB}/Y_{PXR} .

The use of ideal mosaic crystals permit to get essentially bigger radiation yield due to the DB contribution.^{11 12} On this figure there is also a dependence of DB yield for the mosaic sample with $\sigma_m = 1$ mrad and the ratio of DB and PXR yields. It is clear from the figure that even for $T = 0.1$

mm the DB yield from the mosaic crystal is bigger than the yield from perfect one. As the PXR yield, in contrast to radiation spectrum, little depends on the sample mosaicity²⁰, and the DB yield from the perfect crystal is less than PXR yield²¹, a mosaic crystal almost always provides the bigger radiation yield than perfect one. It should be noted that fulfilling the condition $\sigma_m < \vartheta_c$ the DB spectrum is more narrow than PXR spectrum¹², e.g. for $\sigma_m=0.6$ mrad and $T=3.5$ mm the full width of spectrum (on level 10% from max) $\Delta\omega_{DB}=1.2$ keV is less than for the PXR spectrum $\Delta\omega_{PXR}=1.95$ keV, and the relation of intensities ~ 8 .

As it is seen from the figure, the maximum of the PXR and DB yield is reached for the crystal thickness equaled to the absorption path of photons. Due to the increase of the absorption with the decrease of the photon energy the advantage of the mosaic crystals over perfect ones becomes lesser because of the necessity to reduce the crystal thickness. E. g. for $E_c=45$ MeV, silicon crystal and photon energy $\omega \approx 18$ keV the relation of the DB and PXR yields for the target with optimal thickness decreased to ~ 4 ²².

Search or making the samples for the realization of the advantage of the mosaic crystals is another task, that is why let's view what intensity of photon beam can be obtained using widespread and cheap crystals of pyrolytic graphite, mosaicity of which according to the literature varies within $0.2^\circ - 0.5^\circ$. Recently in the work⁶ they proposed the project of the plant for mammography using PXR of electrons in such crystal and showed that such source has a number of advantages over the traditional one based on the electron gun with molybdenum anode.

On Figure 2 there are spectra for the conditions, used in this work: $E_c=35$ MeV, collimation angle 1.24×80 mrad², crystal thickness 10 mm. Angle of the location of the radiated object is $\Theta_D = 2\Theta_B=10.46^\circ$. Curve 1 ($Y = 3.72 \cdot 10^{-6}$ phot./electr.) - the PXR spectrum calculated without taking into account crystal mosaicity. This spectrum is given and discussed in the work⁶. Curve 2 ($Y = 4.70 \cdot 10^{-6}$ phot./electr.) is calculated for $\sigma_m=4$ mrad and for Gaussian distribution of the mosaicity, but without taking into account the diffraction of PXR photons. With this effect $Y = 2.7 \cdot 10^{-6}$ phot./electr. (Curve 3).

It is seen from the figure that mosaicity causes the decrease of the amplitude in the spectrum peak and its shift to the region of lower values of ω , that is caused by the strong dependence of the reflection ability from the photons energy ω ¹³. This factor also causes the bigger PXR yield from the mosaic crystal in comparison with the perfect one. The second diffraction of PXR photons decreases the radiation yield almost twice and shifts

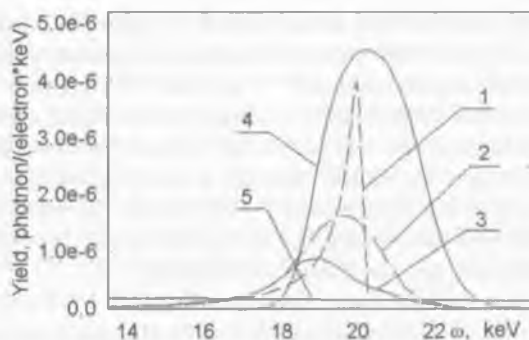


Fig. 2. Radiation spectra in the mosaic crystal of pyrolytic graphite for the conditions of the work⁶: $E_e=35$ MeV, $\Delta\Theta_x\Delta\Theta_y=1.24\times 80$ mrad², $T=10$ mm.

the maximum in the spectrum more, because in the direction of the initial BS beam the photons, with the energy corresponding to maximum in the distribution of mosaic blocks, re-reflect in a bigger extent (see Curve 4).

From the given on the same figure DB spectrum (Curve 4, $Y_{calc} = 1.32 \cdot 10^{-5}$ phot./electr.) it is seen that as for the silicon mosaic crystal the DB yield is much bigger than the PXR yield and the values obtained in the mentioned work. Nevertheless, the width of DB spectrum $\Delta\omega_{DB} \sim 2.86$ keV is bigger than the width of PXR spectrum $\Delta\omega_{PXR} \sim 2.25$ keV and especially bigger than the PXR spectrum from the perfect (not existed in nature) crystal of pyrolytic graphite $\Delta\omega_{PXR} \sim 0.6$ keV, that is caused by bigger value of σ_m in comparison with the collimation angle.

The main problem when we use the crystals with optimal thickness is not the spectrum width but the big BS background in the location of the radiated object. Apparently this is the main reason why the authors' idea⁶ was not realized. From the given on the Figure 2 BS spectrum (Curve 5) it is seen that its contribution is about 3% from the peak amplitude in the DB spectrum.

As BS spectrum stretches right up to the finite electron energy, the number of BS and DB photons, fallen on the radiated object when using the crystals of optimal thickness, as a rule is comparable and the full energy is in some extent bigger than the full energy of useful radiation. E.g. for the silicon crystal with the thickness 3.5 mm and the conditions of the Figure 1 $Y_{DB} \approx 9.4 \cdot 10^{-8}$ phot./electr. and $Y_{BS} \sim 7 \cdot 10^{-8}$ phot./electr. in spite of the fact that its level was lesser than 1 % from the amplitude in the maximum of

DB spectrum, and the full BS energy $W_{BS} \sim 1 \cdot 10^{-4}$ keV/electr. is almost twice orders bigger than the full energy of useful radiation $W_{DB} \approx 3.1 \cdot 10^{-6}$ keV/electron. For the graphite crystal and the conditions⁶ correlation of the full energies is worse because of the bigger BS background. It is clear that using the perfect crystals of optimal thickness and the PXR mechanisms these correlations will be by far worse.

To confirm the adequacy of the given estimations we'll refer to the results of the work²⁴, where the contribution of the background in the crystals of lithium fluoride with the thickness 5.8 mm and 1.55 mm was noticeable even with and the angles of observation $\Theta_D = 30^\circ$ and 60° . It is clear that using the perfect crystals of optimal thickness and the PXR mechanisms these correlations will be worse. The correlation of the background doses and useful radiation, which is defined by the length and the solution of the radiated object, will be less than the correlation of the full energies of radiation and it should be estimated separately.

4. Double-crystal scheme

One of the solution for the problem of high level of background can be a double-crystal scheme. Recently in the work²⁶ the system of two perfect crystals for the PXR generation in a thin crystal and its subsequent diffraction in another, thicker one was realized. Such schemes have been used in double-crystal monochromators¹³. The main advantage of such scheme is that the narrow width of spectrum leads to low intensity of radiation. If the width of the spectrum is not a critical parameter, e.g. for the transmission radiography and K-edge angiography, where $\Delta\omega/\omega \sim 2-3\%$ may be enough, than the use of mosaic crystals instead of the perfect ones can enlarge the radiation yield in some times¹².

The realization of the scheme is rather simple. As in the work²⁶ the electron beam falls on the crystal, placed in a goniometer and unfolded at the angle Θ_B to get the required energy of photons. Produced in the crystal photons pass through the collimator which cuts the necessary area of spectrum and angle distribution and is fixed at the angle $\Theta_D = 2\Theta_B$. Collimated radiation falls on the second crystal, placed in another goniometer and unfolded at the same angle (geometry (n,-n)) and is reflected in the line of the radiated object. To change the energy of photon beam according Bragg's law we should change the orientation of both crystals, the position of the collimator and the second crystal in such a way that the line of the beam of diffracted radiation as before should pass through the radiated object. One of the main advantages of this scheme is that we needn't move

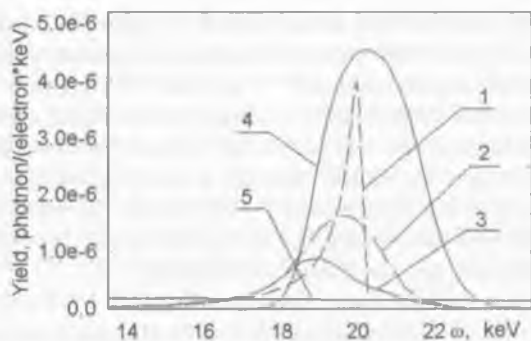


Fig. 2. Radiation spectra in the mosaic crystal of pyrolytic graphite for the conditions of the work⁶: $E_e=35$ MeV, $\Delta\Theta_x\Delta\theta_y=1.24\times 80$ mrad², $T=10$ mm.

the maximum in the spectrum more, because in the direction of the initial BS beam the photons, with the energy corresponding to maximum in the distribution of mosaic blocks, re-reflect in a bigger extent (see Curve 4).

From the given on the same figure DB spectrum (Curve 4, $Y_{calc} = 1.32 \cdot 10^{-5}$ phot./electr.) it is seen that as for the silicon mosaic crystal the DB yield is much bigger than the PXR yield and the values obtained in the mentioned work. Nevertheless, the width of DB spectrum $\Delta\omega_{DB} \sim 2.86$ keV is bigger than the width of PXR spectrum $\Delta\omega_{PXR} \sim 2.25$ keV and especially bigger than the PXR spectrum from the perfect (not existed in nature) crystal of pyrolytic graphite $\Delta\omega_{PXR} \sim 0.6$ keV, that is caused by bigger value of σ_m in comparison with the collimation angle.

The main problem when we use the crystals with optimal thickness is not the spectrum width but the big BS background in the location of the radiated object. Apparently this is the main reason why the authors' idea⁶ was not realized. From the given on the Figure 2 BS spectrum (Curve 5) it is seen that its contribution is about 3% from the peak amplitude in the DB spectrum.

As BS spectrum stretches right up to the finite electron energy, the number of BS and DB photons, fallen on the radiated object when using the crystals of optimal thickness, as a rule is comparable and the full energy is in some extent bigger than the full energy of useful radiation. E.g. for the silicon crystal with the thickness 3.5 mm and the conditions of the Figure 1 $Y_{DB} \approx 9.4 \cdot 10^{-8}$ phot./electr. and $Y_{BS} \sim 7 \cdot 10^{-8}$ phot./electr. in spite of the fact that its level was lesser than 1 % from the amplitude in the maximum of

DB spectrum, and the full BS energy $W_{BS} \sim 1 \cdot 10^{-4}$ keV/electr. is almost twice orders bigger than the full energy of useful radiation $W_{DB} \approx 3.1 \cdot 10^{-6}$ keV/electron. For the graphite crystal and the conditions⁶ correlation of the full energies is worse because of the bigger BS background. It is clear that using the perfect crystals of optimal thickness and the PXR mechanisms these correlations will be by far worse.

To confirm the adequacy of the given estimations we'll refer to the results of the work²⁴, where the contribution of the background in the crystals of lithium fluoride with the thickness 5.8 mm and 1.55 mm was noticeable even with and the angles of observation $\Theta_D = 30^\circ$ and 60° . It is clear that using the perfect crystals of optimal thickness and the PXR mechanisms these correlations will be worse. The correlation of the background doses and useful radiation, which is defined by the length and the solution of the radiated object, will be less than the correlation of the full energies of radiation and it should be estimated separately.

4. Double-crystal scheme

One of the solution for the problem of high level of background can be a double-crystal scheme. Recently in the work²⁶ the system of two perfect crystals for the PXR generation in a thin crystal and its subsequent diffraction in another, thicker one was realized. Such schemes have been used in double-crystal monochromators¹³. The main advantage of such scheme is that the narrow width of spectrum leads to low intensity of radiation. If the width of the spectrum is not a critical parameter, e.g. for the transmission radiography and K-edge angiography, where $\Delta\omega/\omega \sim 2-3\%$ may be enough, than the use of mosaic crystals instead of the perfect ones can enlarge the radiation yield in some times¹².

The realization of the scheme is rather simple. As in the work²⁶ the electron beam falls on the crystal, placed in a goniometer and unfolded at the angle Θ_B to get the required energy of photons. Produced in the crystal photons pass through the collimator which cuts the necessary area of spectrum and angle distribution and is fixed at the angle $\Theta_D = 2\Theta_B$. Collimated radiation falls on the second crystal, placed in another goniometer and unfolded at the same angle (geometry (n,-n)) and is reflected in the line of the radiated object. To change the energy of photon beam according Bragg's law we should change the orientation of both crystals, the position of the collimator and the second crystal in such a way that the line of the beam of diffracted radiation as before should pass through the radiated object. One of the main advantages of this scheme is that we needn't move

most effective for hard photons generation ($\omega > 20$ keV), because the big length of absorption permits to enlarge the thickness of the crystal and the radiation yield. Mosaicity $\sigma_m < \vartheta_c$ provides the increasing of the radiation yield without noticeable worsening of radiation monochromaticity.

2) When using the single-chip scheme the optimal are the crystals with smaller parameter of lattice and maximally acceptable from point of the practical economy electron energy.

3) Traditional scheme of generation of radiation practically is not suitable for the medical purposes because of the big bremsstrahlung background in the position of the irradiated object with using the crystals of optimal thickness and low effectiveness for small thicknesses.

4) Use of mosaic crystals with $\sigma_m \sim 0.2-0.6$ mrad in Laue's geometry instead of the perfect ones in combination-crystal scheme of radiation generation permits greatly enlarge the yield of hard photons with some worsening of monochromaticity.

5) Double-crystal scheme permits to get rid of bremsstrahlung background and improve monochromaticity in comparison with traditional scheme. The additional advantage of such scheme is that you needn't move the irradiated object when changing the photon energy.

The work is fulfilled with partial support of RFBR (grants 05-02-17648 and 09-02-01445) and the programme of inner grants of BelSU.

References

1. V.G. Baryshevskii, I.Ya. Dubovskaia Diffraction phenomena in spontaneous and collective emission of relativistic electrons in crystals, Itogi Nauki Tekh. Ser.: Puchki Zariazhen. Chastits Tverd. Telo, 1991, M.: VINITI, v.4, p.129-225. (in Russian)
2. A.S. Lobko Experimental investigations of parametric X-ray radiation, Mn. BSU, 2006. - 201p. (in Russian).
3. G. Garibian, Shi Yang Quantum microscopic theory of the emission from charged particle moving in a crystal, Sov. Phys. JETP, 1971, v.61, p.930-943.
4. V. Baryshevskii, I. Feranchuk On the transition radiation of gamma-quantum from a crystal, Sov. Phys. JETP, 1971, v.61, p.944-948.
5. P. Baldelli, A. Taibi, A. Tuffanelli, M. Gambaccini Dose comparison between conventional and quasimonochromatic systems for diagnostic radiology, Physics in Medicine and Biology, 2004, v.49, p.4125-4146
6. M.A. Peistrup, Wu Xizing, V.V. Kaplin, S.R. Uglov, J.T. Cremer, D.W. Rule, R.B. Fiorito A design of mammography units using a quasimonochromatic x-ray source, Review of Scientific Instruments (2001) v.72, No. 4, p.2150-2170
7. Y. Takashima, K. Aramitsu, I. Endo et al. Observation of monochromatic

- and tunable hard X radiation from stratified Si single crystals, Nucl. Instr. and Meth. in Phys. Res., 1998, v.B145, p.25-30.
8. J. Freudenberger, E. Hell, W. Knupher Perspectives of medical X-ray imaging, Nucl. Instr. and Meth. 2001. V.A466, p. 99-104.
 9. V.V. Kaplin., S.R. Uglov, V.N. Zabaev, M.A. Piestrup, C.K. Gary Observation of bright monochromatic x rays generated by relativistic electrons passing through a multilayer mirror , Appl. Phys. Lett. 76 (2000), p.3647-3649.
 10. V.V. Kaplin, S.R. Uglov, O.F. Bulaev, V.J. Goncharov, A.A. Voronin, M.A. Peistrup, C.K. Gary, N.N. Nasonov, M.K. Fuller Tunable, monochromatic x rays using the internal beam of a betatron , Applied Physics Letters (2002), V.80, No. 18, p.3427-3429
 11. E.A. Bogomazova, B.N. Kalinin, G.A. Naumenko, D.V. Padalko, A.P. Potylitsyn, A.F. Sharafutdinov and I.E. Vnukov Diffraction of real and virtual photons in a pyrolytic graphite crystal as source of intensive quasimonochromatic X-ray beam , Nucl. Instr. and Meth. in Phys. Res., 2003, B201, p.276-291
 12. A.N. Baldin, I.E. Vnukov, R.A. Shatokhin Using mosaic crystals for the generation of intense X-ray beam , Technical Physics Letters, 2007, v.33, p.625-628.
 13. R. James The optical principles of the diffraction of X-rays G. Bell and Sons, London, 1958, 464p.
 14. K.-H. Brenzinger, B. Limburg, H. Backe et al. How narrow is the linewidth of parametric X-ray radiation , Phys. Rev. Lett. 1997. V.79. p.2462-2465.
 15. H. Nitta Kinematical theory of parametric X-ray radiation , Phys. Lett., 1991, A158, p.270-274.
 16. D.T. Cromer and J.T. Waber Scattering factors computed from relativistic Dirac-Slater wave functions , Acta Cryst. 1965, v.18, p.104-109.
 17. A. Potylitsin Influence of Beam Divergence and Crystal Mosaic Structure Upon Parametric X-Ray Radiation Characteristics, arXiv:cond-mat/9802279 v1 26 Feb 1998.v1 26 Feb 1998.
 18. V.A. Bazylev, N.K. Zhevago, Radiation of Relativistic Particles in External Fields and in Matter (Nauka Pub., Moscow, 1987, 272p.)(in Russian).
 19. M. Chabot, P. Nicolai, K. Wohrer, J.P. Rozet, A. Touati, A. Chetoui, D.Vernhet and M.F. Politis, X-ray reflectivities, at low and high order of reflection, of flat highly oriented pyrolytic graphite crystals , Nucl. Instr. and Meth. in Phys. Res., 1991, B61, p.377-384.
 20. A.M. Afanas'ev and M.A. Aginian Radiation of ultrarelativistic particles under penetration across perfect and mosaic crystals , Sov. Phys. JETP, 1978, v.74, p.300-309.
 21. D.A. Baklanov, A.N. Baldin, I.E. Vnukov, D.A. Nechaenko, R.A. Shatokhin Related contribution of diffracted bremsstrahlung and parametric X-ray radiation in perfect crystals , The Journals of Kharkiv National University, Physical series "Nuclei, Particles, Fields", 2007, v.763, No.1(33), p.41-56.(in Russian).
 22. A.N. Baldin, I.E. Vnukov, D.A. Nechaenko, R.A. Shatokhin Influence of crystal mosaicity on characteristics of parametric X-ray radiation , The Journals

- of Kharkiv National University, Physical series " Nuclei, Particles, Fields", 2007, v.744, No.3(31), p.51-65.(in Russian).
23. R.B. Fiorito, D.W. Rule, X.K. Maruyama et al. Observation of higher order parametric x-ray spectra in mosaic graphite and single silicon crystals, *Phys.Rev.Lett.* 1993, V.71, p.704-707.
 24. B. Sones, Y. Danon, R.C. Block Lithium fluoride (LiF) crystal for parametric X-ray (PXR) production. , *Nucl. Instr. and Meth. in Phys. Res. B.* 2005, V.227, p.22-31.
 25. Z. Pinsker *Dynamical Scattering of X-rays in Crystals*, Berlin, Springer, 1984, 394p.
 26. Y. Hayakawa, I.Sato, K. Haykawa, T. Tanaka, A. Mori,T. Kuwada, T.Sakai, K. Nogami, K. Nako, T. Sakae Status of the parametric X-ray generator at LEBRA. Nihon University , *Nucl. Instr. and Meth. in Phys. Res.*, 2006, B252, p.102-110.